From imperfect to perfect $Bi_2Sr_2CaCu_2O_x$ (Bi–2212) grains

B. Heeb and L. J. Gauckler
Nichtmetallische Werkstoffe, ETH Zürich, Sonneggstr.5, CH-8092 Zürich, Switzerland

H. Heinrich and G. Kostorz
Institut für Angewandte Physik, ETH Hönggerberg, CH-8093 Zürich, Switzerland

(Received 20 February 1993; accepted 23 April 1993)

The 2212 phase formation during annealing of melt textured Bi–2212 ($Bi_2Sr_2CaCu_2O_x$) was investigated using differential thermal analysis, thermal gravimetric analysis, x-ray diffraction, scanning electron microscopy, energy dispersive x-ray analysis, and high resolution transmission electron microscopy. After zone melting, the material is multiphase consisting of 2212, 2201, $Sr_{1-x}Ca_xCuO_2$, and the eutectic. The 2212 phase formed is highly perfect with less than 5% intergrowths of 2201 layers; the 2201 phase shows no intergrowth of 2212 at all. In the first period of the annealing, remelting of the eutectic leads to fast oxygen diffusion and a high 2212 formation rate. The 2201 → 2212 transformation proceeds via intermediate states of high defect density. The 2212 grains contain up to 30–70% 2201 intergrowths. Further heat treatments lead to an annihilation of the great majority of intergrown 2201 layers. We propose a model for the formation of 2212 grains with a low planar defect density, based on frequent stacking faults, that allows diffusion of Ca- and Cu-atoms over a short distance. The model provides a schematic description of this solid-state process and correlates it to the characteristic microstructural features of melt-processed Bi–2212.

I. INTRODUCTION

Bi–2212 ($Bi_2Sr_2CaCu_2O_x$) is mainly produced by melt processing, e.g., partial melting of thick films[1] or zone melting of bulk samples.[2,3] These processing routes enable the formation of a highly textured, weak link-free microstructure, giving the material the potential for utilization in a variety of applications that require the conduction of high dissipation-free currents.

However, the processing routes via a liquid phase are seriously complicated by the incongruent melting of Bi–2212. This is due to oxygen loss during heating and melting. As a consequence of insufficient equilibration of this oxygen deficiency during solidification, the microstructure of nominal 2 : 2 : 1 : 2 composition is multiphase containing 2201, $Sr_{1-x}Ca_xCuO_2$ ($x = 0.4$), Cu-free phases, and Cu_2O as impurity phases.[4,5] This occurs especially in bulk material due to the long diffusion distances, in thick films only at high cooling rates due to the short diffusion time. Annealing the as-solidified material at temperatures higher than 800 °C is necessary and yields a high amount of the 2212 phase with good superconducting properties.[3] The formation of the two-layer compound proceeds in two steps, which were explained by solid/liquid and subsequent solid/solid reactions of the secondary phases with 2201.[5] During the first hours of the annealing a considerable weight increase is observed, which is attributed to oxygen absorption.[6]

After annealing the Bi–2212 phase still contains grains with a high concentration of crystal defects. They have been extensively characterized by transmission electron microscopy (TEM) investigations.[7–10] Especially the intergrowth of half-cells of 2201 in 2212 grains is often observed in melt processed as well as in sintered samples.[7,9,11–13] These intergrowths may either indicate an incomplete 2201 → 2212 transformation,[9] or be a possibility of the accommodation of the chemical composition.[13] Little information is available about the amount and distribution of the intergrowths within the grains. In general, their amount was found to be increased in samples of Bi-rich starting compositions.[13] Furthermore, they are frequently found at twin boundaries, and their insertion is thought to be a possible mechanism for solid-state diffusion parallel to the c-axis.[9] Lang *et al.*[11] reported that the alternate arrangement of the half-cells of 2201 and 2212 is slightly preferred; only few identical half-cells are nearest neighbors.

The purpose of this work is to clarify the formation of the 2212 phase in melt textured bulk material during annealing at 850 °C in air. Special emphasis is given to microstructural changes concerning the amount and distribution of 2201 intergrowths in 2212 grains at different annealing times.

II. EXPERIMENTAL

Starting material was single phase Bi–2212 powder (Hoechst High Chem, Frankfurt, Germany) with an average grain size of 15–20 μm (grade 3, chemical purity 99.7%). The powder was pressed into Al_2O_3

crucibles (200 × 20 × 10 mm^3) and zone molten in air at a pulling rate of 3 mm/h. The maximum temperature in the melt was 930 °C. The temperature gradient at the solidification front at 890 °C was measured to be 10^4 K/m. After zone melting the sample was cut into several pieces of 15 × 10 × 5 mm^3 and annealed at 850 °C in air for various periods of time up to 100 h. After the annealing, the samples were cooled in air.

The samples were investigated by x-ray diffraction (XRD) with Cu K_α radiation using Si as the internal standard, and scanning electron microscopy (SEM). Chemical compositions of the phases were determined by energy-dispersive x-ray analysis (EDX) (Tracor-Northern Series II, Wisconsin) at an acceleration voltage of 25 kV with a Si (Li) detector. The ZAF correction[5] was applied to the intensities of the Bi M_α, Sr L_α, Ca K_α, and Cu K_α lines, and the compositions were calculated by means of internal standards. The accuracy was checked by a sintered single phase $Bi_{2.1}Sr_{2.0}Ca_{1.0}Cu_{2.0}O_x$ sample and found to be better than ±3 at. %.

TEM specimens were prepared by mechanical polishing, thinning with a dimple-grinder, and ion-milling to perforation in an Ar beam. A Philips CM30 (C_s = 1.1 mm, LaB_6-cathode) at 300 kV was used for HRTEM, electron diffraction (ED), and EDX.

The annealing of an as-grown sample was independently carried out in a differential thermal analysis (DTA) and thermal gravimetric analysis (TGA) experiment. The sample (724 mg) was heated at the rate of 5 K/min to 850 °C in air and equilibrated for 85 h. The accuracy of the weight measurement is ±0.025 mg.

The chemical compositions of the phases are written as abbreviations. The notations are as follows: the order of the elements is Bi/Sr/Ca/Cu and the letter x is used for the Sr/Ca exchange. For example, the chemical composition of the phase called "01x1" is $Sr_{1-x}Ca_xCuO_2$.

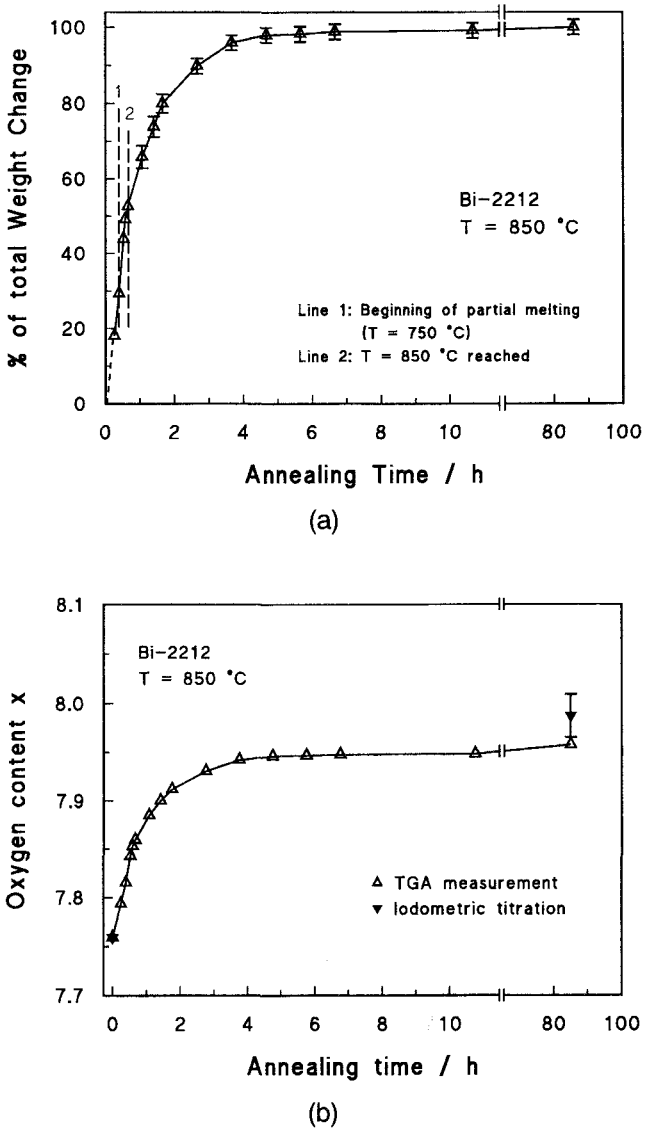

FIG. 1. (a) Weight change of zone molten Bi–2212 ($Bi_2Sr_2CaCu_2O_x$) as a function of the annealing time in air at 850 °C. 100% corresponds to a weight increase of the as-grown sample of 2.59 mg = 0.36%. (b) Oxygen content x of zone molten Bi–2212 as a function of the annealing time in air at 850 °C. The results of the TGA measurement, as well as those of the iodometric titration, are shown.

III. RESULTS AND DISCUSSION

A. Oxygen diffusion during annealing

After zone melting the samples were oxygen deficient owing to oxygen loss during melting and their suppressed reoxidation during cooling. Therefore, annealing in air at 850 °C led to a considerable weight increase, which was measured in the DTA/TGA experiment. Figure 1(a) shows the weight change of the as-grown sample as a function of the annealing time. The weight increase was very fast, as already reported in the literature,[6] and was completed to about 99% after 10 h. It was attributed to the oxygen diffusion into the sample. Two additional observations should be mentioned.

(1) The weight increase started already during heating at temperatures above 600 °C. This point was then chosen at t = 0 for the annealing time. The final heat-treatment temperature of 850 °C is reached after 40 min, as shown in Fig. 1(a).

(2) Melting of one of the phases could be detected as low as 750 °C by an endothermic signal in the DTA. This temperature is in excellent agreement with the solidification temperature of the eutectic consisting of Cu_2O and $Bi_2Sr_2CaO_x$ ($23x0, x$ = 1), as reported previously.[5,14] The occurrence of this oxygen-deficient liquid phase enhanced the oxygen diffusion. The liquid might still be present during the first hours of the annealing at 850 °C and, therefore, facilitated the fast oxygen absorption of the sample.

Therefore, we conclude that within the first 6–10 h of the annealing the fast formation of the two-layer compound is due to the presence of a liquid phase facilitating the mobility of oxygen, as well as the 2212 formation.

Before and after the annealing in the DTA apparatus, the total oxygen content of the sample was measured by iodometric titration.[15] The oxygen content expressed by x in the formula unit $Bi_2Sr_2CaCu_2O_x$ of the as-grown sample was $x = 7.76 \pm 0.003$ and after the heat treatment $x = 7.99 \pm 0.022$, respectively, as shown in Fig. 1(b). This value is considerably below the optimum oxygen index of single phase Bi–2212 of about 8.2. However, after the annealing, the samples still consisted of several phases. Concerning the 2212 phase fraction, ac-susceptibility measurements showed a T_c of 91 K after annealing, indicating that the oxygen index of the two-layer phase in the samples was near the optimum value. The low overall oxygen index of the sample can therefore be considered as a consequence of oxygen-poor secondary phases ($01x1, 02x1$). Additionally, the weight changes of the TGA measurements were calculated into changes of the oxygen content of the sample and added to the starting value of 7.76. The result is also shown in Fig. 1(b). The calculated end value after 85 h of annealing was 7.96, in good agreement with the titration experiments.

B. Transformation 2201 → 2212 during annealing

The 2212 phase formation is discussed in the following three sections. In the first one the microstructure of the material directly after the zone melting process is described (so-called "as-grown" sample). This highly nonequilibrated state fixes the starting point of the annealing experiments. The second section describes the microstructure and phase development during the first 10 h of the heat treatment, as most of the oxygen absorption occurs then. The last section provides information about the long-term annealings (20 to 100 h). During this latter part of the annealings, the microstructural changes are mainly on the nanometer scale, i.e., inside the grains. All the results of the EDX, XRD, and HRTEM experiments are summarized in Table I. In addition, the fraction of 2201 half-cells in the 2212 grains as a function of the annealing time at 850 °C is shown in Fig. 2. The details of the figure will also be discussed in the following sections.

Processing with alumina crucibles is known to lead to contamination of the samples with Al impurities.[5,16] However, Al was never found in any of the superconducting phases but is incorporated into Sr–Ca–Al–O precipitates of a composition near $SrCa_2Al_2O_x$, as revealed by EDX. This phase is isostructural with $Sr_3Al_2O_x$.[17] Moreover, TEM/EDX investigations showed an Al-containing phase with the composition 361.51 (Al =1). This phase was described elsewhere.[12]

1. As-grown sample

The as-grown sample after zone melting was multiphase containing $01x1$, 2201, and 3430 as secondary

TABLE I. Chemical composition and intergrowth concentration of the 2212 grains and the secondary phases of melt textured Bi–2212 as a function of annealing time in air at 850 °C.

Annealing time/h	Chemical composition of the 2212 phase[a] Bi/Sr/Ca, Cu = 2	2201 intergrowths in the 2212 grains/%[b] average	2201 intergrowths in the 2212 grains/%[b] single grains	Secondary phases[c]
0	2.30/2.02/0.74 ±0.47/±0.26/±0.12	6	2–21	2201 (m)[d], $01x1$ (m), 3430 (m)
10	2.02/2.09/0.85 ±0.04/±0.13/±0.06	17	2–9	$01x1$ (m), 3430 (vw)
	2.27/2.10/0.90 ±0.90/±0.10/±0.09		28–71	
20	2.23/2.07/0.87 ±0.11/±0.07/±0.05	8	2–17	$01x1$ (m), 3430 (vw)
40	2.22/2.04/0.94 ±0.06/±0.08/±0.04	...	...	$01x1$ (m)
60	2.07/2.07/0.85 ±0.07/±0.06/±0.07	...	...	$01x1$ (m)
80	...	...	5–8	$01x1$ (m)
100	2.10/2.04/0.86 ±0.08/±0.10/±0.09	6	0–10	$01x1$ (m)

[a]EDX measurements: average of 6–10 point analyses.
[b] HRTEM measurements: statistics of approximately 2000 to 6000 half-cells.
[c]X-ray diffraction analysis.
[d]Chemical composition of 2201: 1.85/1.39/0.19/1.

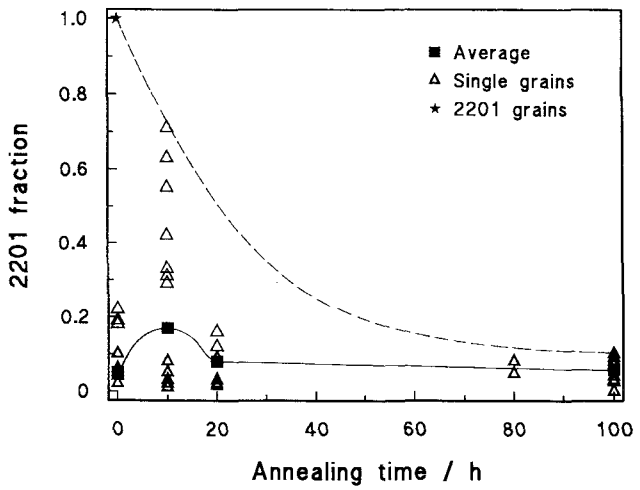

FIG. 2. Fraction of 2201 intergrowths in the 2212 grains of zone molten Bi–2212 as a function of the annealing time at 850 °C in air. The average of all investigated 2212 grains (■), as well as the fraction in single 2212 grains (△), are shown. "2212" grains with a 2201 fraction of 1 correspond to perfect 2201 grains (★).

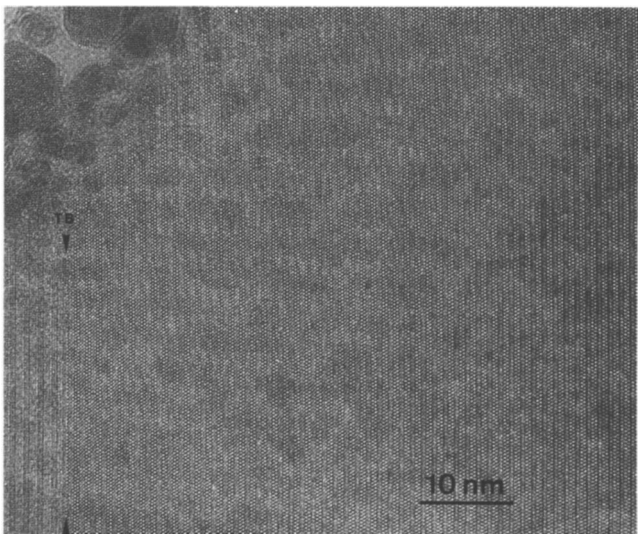

FIG. 3. [110]-HRTEM of a 2201 grain in the as-grown sample. On the left side of the figure there is a twist boundary (TB) to a 2212 grain.

phases besides the 2212 phase as determined by XRD. The volume fraction of 2212 was 40%. The formation of the 2212 grains was due to the slow solidification rate of about 30 K/h during zone melting. It could proceed at least partially in the presence of a liquid. The EDX measurements showed a wide scattering of the chemical composition of the 2212 phase, indicating the time period for the 2212 formation to be insufficient to reach the equilibrium state. On the other hand, HRTEM showed that some of the 2212 grains contain on an average only 6% of intergrowths of 2201 half-cells (see Fig. 2). This fraction corresponds to the amount at the end of the post-solidification heat treatment, as will be shown later.

The volume fraction of the 2201 phase was 20–30 vol. %. In contrast to the 2212 grains, the 2201 crystallites are always perfect without any intergrowths of the two- or three-layer compound. They therefore correspond to the "2212" grains with a 2201 fraction of 1 in Fig. 2. Such a perfect 2201 grain is shown in Fig. 3.

2. Short-time annealing (<10 h)

The first 10 h of post-solidification heat treatment caused strong changes in the microstructure. Concerning the secondary phases, XRD measurements showed that during the fast oxygen uptake assisted by the liquid phase and the increase of the volume fraction of the 2212 phase, the 2201 and Cu-free phase disappeared almost completely. In Fig. 4 this microstructural change is pointed out by the XRD patterns of the samples before and after 10 h of annealing.

EDX measurements of the 2212 grains showed that they are rich in Bi and Sr (or poor in Ca and Cu) compared to the ideal 2 : 2 : 1 : 2 stoichiometry. The chemical compositions of the different grains can be grouped around two compositions. One composition, 2.3/2.1/0.9/2, is specifically rich in Bi and Sr; the other with 2.0/2.1/0.9/2 is less enriched in Bi and Sr, but is still higher in Sr compared to ideal 2212. As the one-layer compound with composition 1.9/1.4/0.2/1 has a higher (Bi + Sr) : (Ca + Cu) ratio than the 2212 phase, the Bi- and Sr-excess in the grains can be explained by different amounts of 2201 half-cell intergrowths. The deviations from ideal 2 : 2 : 1 : 2 stoichiometry would then correspond to 30% and 3% 2201 intergrowths, respectively.

To corroborate this suggestion the two kinds of 2212 grains were carefully analyzed by HRTEM to gain information about the defect density. The following results were obtained: (1) There are grains with a small amount (≈5%) of 2201 intergrowths. These grains seem to have already reached the quasiequilibrium, as discussed earlier. (2) A second population of 2212 grains with a large amount of intergrowths (30–70%) was detected (Fig. 5). The defects are not distributed uniformly within the grains. We can find regions with high and regions with low intergrowth densities in the same grain. (3) No pure 2201 grains were detected by TEM, but in some 2212 grains there are regions with more than five consecutive 2201 layers.

The above results can be summarized as follows. The solid/liquid reaction during the first few hours of the annealing at 850 °C leads to a fast 2201 → 2212 transformation. If it is incomplete, the 2212 grains show a large amount of planar defects. The EDX measurements were corroborated by the HRTEM results. The different chemical compositions of the grains measured by the

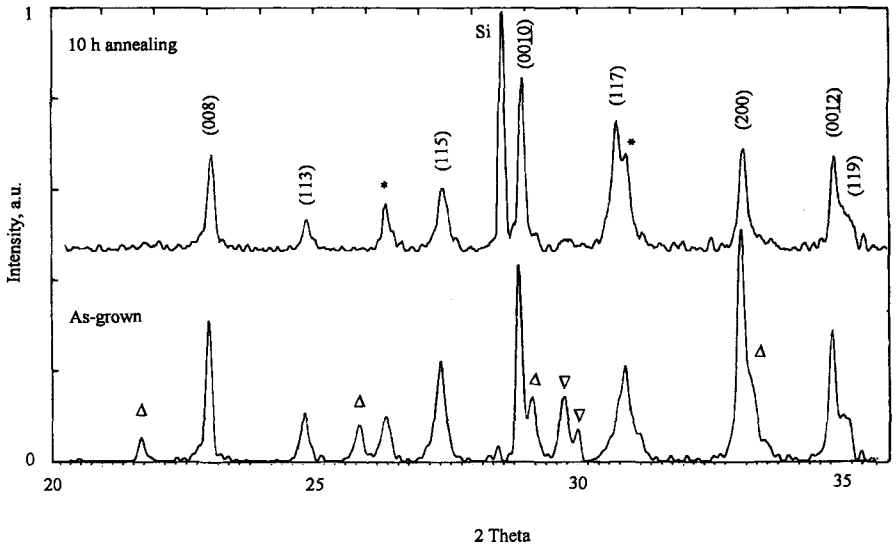

FIG. 4. XRD patterns of the as-grown sample (lower part) and after 10 h of annealing in air at 850 °C (upper part). The 2212 peaks are indexed; impurity phases: (△) one-layer phase; (▽) 3430; (*) 01x1.

EDX correlate well with the markedly large amount of 30–70% intergrowths. The second kind of 2212 grains are the defect-poor grains, which were already observed in the as-grown sample. Their slight Bi and Sr excess (or the slight Ca and Cu deficiency) measured by EDX can be attributed to an average of 5% intergrowths of 2201 half-cells.

3. Long-time annealing (10–100 h)

The reaction during this period of the annealing took place with hardly any additional oxygen absorption; the weight increase was less than 1% of the total amount (see Fig. 1). The quantitative phase analysis showed a dramatic decrease of the formation kinetics of the 2212 phase.[2] We attributed these observations to a change in the reaction mechanism from a solid/liquid to a solid-state reaction after about 10 h of annealing. However, despite little changes in overall phase compositions, considerable changes inside the grains of the 2212 phase occurred.

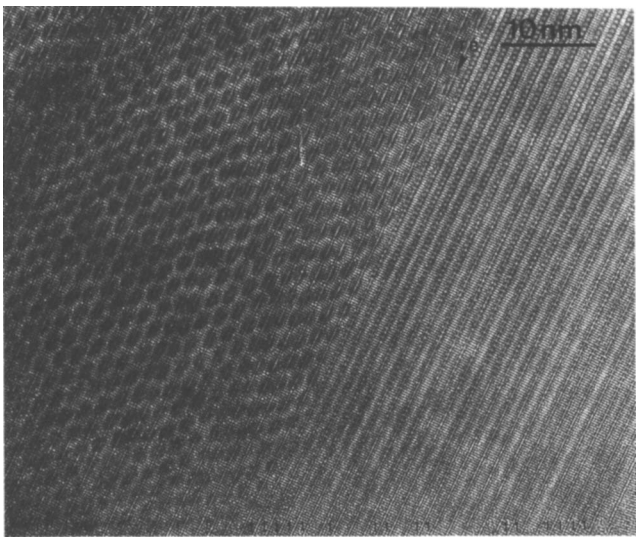

FIG. 5. HRTEM of a 2212 grain after 10 h of annealing showing a high density of 2201 intergrowths on the right side ([010]-orientation). There is a 90° twist boundary (TB) to the left side ([100]-orientation) with a low density of 2201 intergrowths.

The 2212 grains of the samples after 20 and 100 h of annealing were carefully investigated by HRTEM. The amount of 2201 intergrowths decreased considerably from 30–70% after 10 h to 0–10% after 100 h of annealing (see Fig. 2). Furthermore, the difference between single grains got considerably smaller; i.e., hardly any crystallite with more than 10% intergrowths could be detected. The intergrowths of the 2201 half-cells were often concentrated after 100 h near grain and twist boundaries, indicating that the defects in the inner part of the grains vanished first. In Fig. 6 a 2212 grain after 100 h of annealing is shown with 2201 intergrowths piled up at a twist boundary.

C. Model for the 2201 → 2212 transformation

To explain this microstructural development during the solid-state reaction, the model shown schematically in Fig. 7 is proposed. The starting situation is shown in Fig. 7(a) with the (010) plane of a 2212 grain and an intergrowth of a half-cell of 2201. The tendency of the 2201 and 2212 phase to separate should lead this defect to move through the grain. If a stacking fault is introduced at the grain boundary, the Ca and Cu atoms can diffuse from the adjacent 2212 to the 2201 half-cell over very short distances [Fig. 7(b)]. Such stacking faults

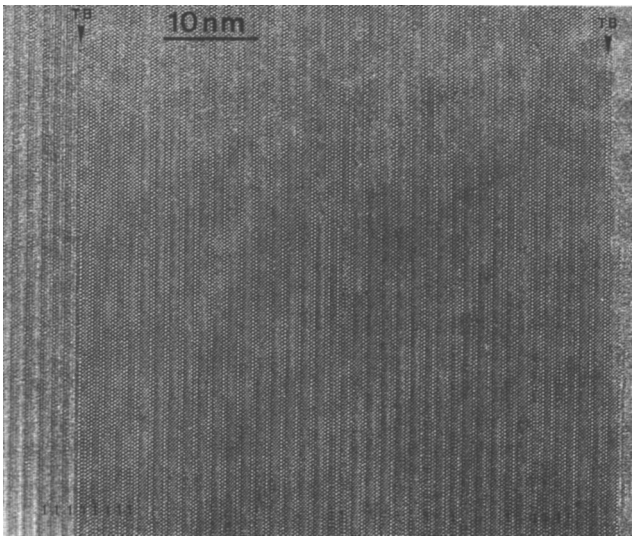

FIG. 6. [110]-HRTEM of a twist boundary in a 2212 grain showing the concentration of 2201 half-cells at the left twist boundary.

in the middle of a 2212 grain were often found, as shown in Fig. 8. Their occurrence was reported previously by Eibl.[8,9] He also suggested that the insertion of stacking faults is a possible mechanism for the diffusion in the c-direction. Indeed, moving this fault once through the grain, the intergrowth is pushed in the direction of the c-axis toward the grain boundary [Fig. 7(c)]. By creating further stacking faults the process can be repeated.

Stacking faults are observed either as single [as described in Figs. 7(a)–7(c)] or as multiple stacking faults. Such a multiple stacking fault is shown in Fig. 8. Single stacking faults can occur only between two adjacent half-cells of different types. Multiple stacking faults can be found in a sequence of 2201 layers. Their movement results in a shift in the c-direction of the whole sequence.

In addition, the 2201 intergrowths can be transformed into 2212 half-cells by enhanced Ca and Cu diffusion at grain boundaries. Especially at boundaries with grains of Ca- and Cu-rich impurity phases (for example Sr–Ca-cuprates) cation diffusion over short distances can lead to defect-free grains and grain boundaries. Excess Ca and Cu cations, transported via diffusion, are then responsible for the decrease of the amount of 2201 intergrowths in the 2212 grains during the long-term annealing.

IV. CONCLUSIONS

The 2212 phase formation during annealing in air at 850 °C in zone molten Bi–2212 was clarified by combination of TGA, XRD, EDX, and HRTEM experiments. 2212 may form via two different processes:

Solid/liquid reaction: The liquid forms owing to the remelting of the eutectic of Cu_2O and $Bi_2Sr_2CaO_x$ ($23x0, x = 1$) in the multiphase, oxygen-deficient as-

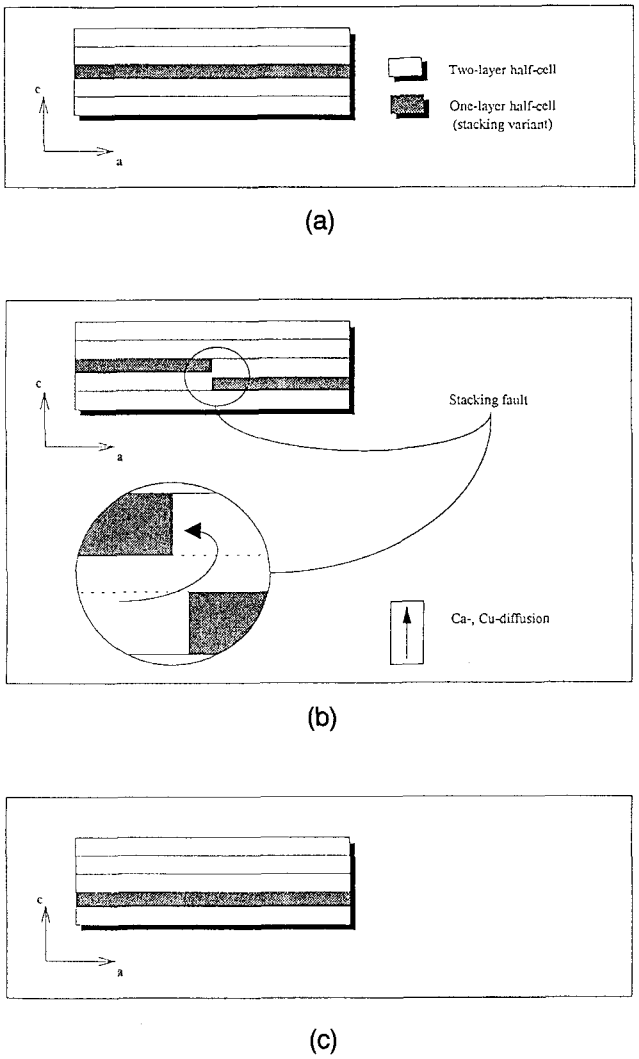

FIG. 7. Model for the movement of the 2201 intergrowths in the 2212 grains: (a) 2212 grain with one half-cell of 2201 (dark). (b) Stacking fault in the 2212 grain enables short distance Ca and Cu diffusion; the stacking variant is pushed toward the grain boundary in the bottom. (c) After the movement of the stacking fault through the whole 2212 grain, the 2201 half-cell has been moved by one half-cell.

grown samples. It enhances the mobility of oxygen leading to a fast oxygen gain, high cation diffusion rate, and leads to a rapid 2212 phase formation. The solid/liquid process lasts during the first few hours of the annealing, at 850 °C less than 10 h. After complete solid/liquid reaction the 2212 grains contain approximately 5% 2201 intergrowths of half-cells of the one-layer compound. Therefore, these grains are slightly richer in Bi and Sr than the ideal 2/2/1/2 stoichiometry. If the solid/liquid reaction is incomplete, up to 70% intergrowths are included in the 2212 grains. No 2201 grains are found after 10 h of annealing.

Solid state reaction: After consumption of the liquid the microstructure consists to a great extent of 2212 grains with very few 2201 intergrowths, of 2212 grains

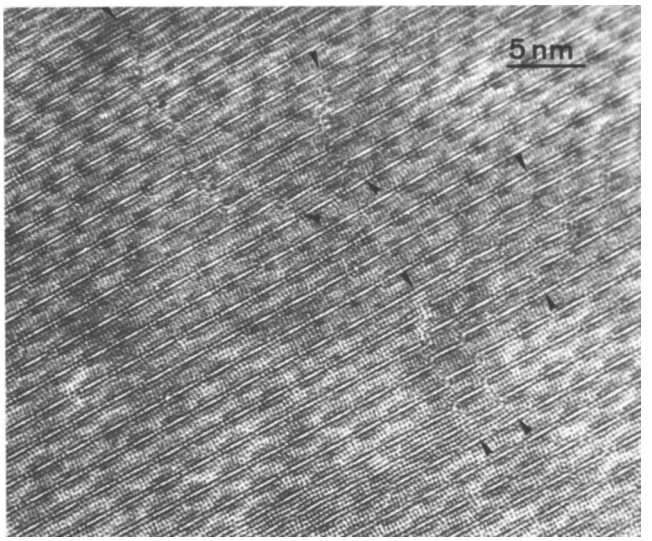

FIG. 8. [100]-HRTEM of a 2212 grain with a high concentration of stacking faults (marked by arrows).

with large Ca and Cu deficiency accompanied by a high defect density, and of the coarse Bi-free primary phase $01x1$. The subsequent solid/solid reaction leads to a decrease of the concentration of 2201 intergrowths in the imperfect 2212 grains. Most 2212 grains reach a quasiequilibrium state with about 5% intergrowths after 100 h of annealing. The creation of stacking faults at grain boundaries and their movement through the grains facilitates cation diffusion parallel to the c-axis. At grain boundaries, the 2201 half-cells can be transformed to 2212 half-cells requiring only very short diffusion distances for Ca and Cu. This is particularly favored at $2212/01x1$ grain boundaries.

The occurrence of the stacking faults may additionally be important in connection with pinning. Since intergrowths as planar defects are always parallel to the CuO_2-planes and for most applications the Lorentz force will act along these planes, they will not be effective as pinning centers. However, the stacking faults, because of the interruption of the intergrowths, may be good pinning centers.

ACKNOWLEDGMENT

Financial support from the Swiss National Science Foundation is gratefully acknowledged.

REFERENCES

1. J. Kase, K. Togano, H. Kumakura, D. R. Dietderich, N. Irisawa, T. Morimoto, and H. Maeda, Jpn. J. Appl. Phys. **29**, L1096–L1099 (1990).
2. Y. Kubo, K. Michishita, Y. Higashida, M. Mizuno, H. Yokoyama, N. Shimizu, E. Inukai, N. Kuroda, and H. Yoshida, Jpn. J. Appl. Phys. **28**, L606–L608 (1989).
3. W. Paul, B. Heeb, Th. Baumann, M. Guidolin, and L. J. Gauckler, in *Layered Superconductors: Fabrication, Properties and Applications*, edited by D. T. Shaw, C. C. Tsuei, T. R. Schneider, and Y. Shiohara (Mater. Res. Soc. Symp. Proc. **275**, Pittsburgh, PA, 1992), pp. 383–387.
4. J. Bock and E. Preisler, *High-Temperature Superconductors: Materials Aspects*, edited by H. C. Freyhardt, R. Flükiger, and M. Peuckert (DGM, Oberursel, 1991), pp. 215–226.
5. B. Heeb, S. Oesch, P. Bohac, and L. J. Gauckler, J. Mater. Res. **7**, 2948–2955 (1992).
6. H. M. Chow, X. P. Jiang, M. J. Cima, J. S. Haggerty, H. D. Brody, and M. C. Flemings, J. Am. Ceram. Soc. **74**, 1391–1396 (1991).
7. Z. Xu, P. D. Han, L. Chang, A. Asthana, and D. A. Payne, J. Mater. Res. **5**, 39–45 (1990).
8. O. Eibl, Physica C **168**, 239–248 (1990).
9. O. Eibl, Physica C **168**, 249–256 (1990).
10. H. W. Zandbergen, W. A. Groen, F. C. Mijlhoff, G. van Tendeloo, and S. Amelinckx, Physica C **156**, 325–354 (1988).
11. Ch. Lang, B. Hettich, M. Schwarz, H. Bestgen, and S. Elschner, Physica C **182**, 79–88 (1991).
12. H. Heinrich, G. Kostorz, B. Heeb, R. Müller, T. Schweizer, and L. J. Gauckler, Ultramicroscopy. **49**, 265–272 (1993).
13. T. G. Holesinger, D. J. Miller, L. S. Chumbley, M. J. Kramer, and K. W. Dennis, Physica C **202**, 109–120 (1992).
14. J. Bock, S. Elschner, and E. Preisler, *Advances in Superconductivity III*, edited by K. Kajimura and H. Hayakawa (Springer, Tokyo, 1991), pp. 797–800.
15. J. T. S. Irvine and C. Namgung, J. Solid State Chem. **87**, 29 (1990).
16. T. G. Holesinger, D. J. Miller, and L. S. Chumbley, J. Mater. Res. **7**, 1658–1671 (1992).
17. Phase Diagrams for Ceramists, Nat. Bur. Stand., Am. Ceram. Soc., **VI**, No. 6427, 136 (1987).